Direct comparison of the flame inhibition efficiency of transition metals using metallocenes

Yusuke Koshiba [a, *], Saori Agata [b], Tomohide Takahashi [b], Hideo Ohtani [c]

[a] Department of Materials Science and Chemical Engineering, Faculty of Engineering, Yokohama National University, 79-5 Tokiwadai, Hodogaya-ku, Yokohama 240-8501, Japan

[b] College of Engineering, Yokohama National University, 79-5 Tokiwadai, Hodogaya-ku, Yokohama 240-8501, Japan

[c] Department of Safety Management, Faculty of Environmental and Information Sciences, Yokohama National University, 79-7 Tokiwadai, Hodogaya-ku, Yokohama 240-8501, Japan

*Corresponding author: Telephone number: +81-45-339-3985

Fax number: +81-45-339-3985

E-mail address: ykoshiba@ynu.ac.jp

Complete postal address: 79-5 Tokiwadai, Hodogaya-ku, Yokohama 240-8501, Japan

Abstract

This study aimed to directly and systematically compare the flame inhibition abilities of various transition metals, including vanadium, ruthenium, osmium, chromium, manganese, iron, cobalt, and nickel, by using the corresponding metallocenes: vanadocene, ruthenocene, osmocene, chromocene, manganocene, ferrocene, cobaltocene, and nickelocene. The downward flame spread rates over filter paper samples on which each metallocene was adsorbed were measured. In addition, thermogravimetric measurements were carried out to finally determine the phase in which each metallocene produced its flame inhibition effect. The results indicated that all these metallocenes, with the exception of vanadocene, exhibit a flame inhibition effect solely in the gas phase, whereas vanadocene shows fire suppression ability in the solid phase. This work also found that, in terms of their fire suppression abilities, the transition metals can be ranked in the following order: Cr > Mn > Fe > Co > Ni > (V >) Os > Ru.

Keywords: Flame inhibition, Metallocene, Transition metal, Flame spread rate, Kissinger method

1. Introduction

Accidental deaths due to fire in Japan average approximately 2000 a year and hence the development of high-performance fire extinguishing agents are required as a means of preventing such loss of life. Transition metals exhibit a wide range of oxidation states, thereby enabling these materials to scavenge radicals present in the chain reactions within flames, and this implies that transition metal compounds should exhibit highly efficient fire-extinguishing capabilities [1–4]. Among the various transition metal compounds, it is well known that iron pentacarbonyl ($Fe(CO)_5$) is a good flame inhibitor [5, 6] and thus this chemical has been proposed as an alternative to the halons. $Fe(CO)_5$, however, is highly toxic [7] and this seriously limits its application as a fire extinguishing agent. In contrast, ferrocene ($FeCp_2$, see Fig. 1), which is also an iron coordination compound, has received much attention because of its good fire suppression performance and low toxicity [8]. A number of studies have been reported on the fire suppression abilities of transition metal salts having different counter ions [9]; however, the suppression abilities of the various transition metal compounds cannot be directly compared from the resulting data. This is because the counter ions, including chloride and bromide, also possess some fire suppression ability and the physical and chemical properties of the transition metal compounds may greatly vary depending on their counter ions.

In order to circumvent this problem and directly compare the suppression ability of transition metals, we have examined the suppression effects of transition metals by using metallocenes (MCp_2) such as chromocene ($CrCp_2$), manganocene ($MnCp_2$), ferrocene, cobaltocene ($CoCp_2$), and nickelocene ($NiCp_2$) [10]. The major advantages of using these metallocenes are that (1) these compounds form a homologous series, (2) the oxidation states of their central metals are identical (i.e., +2), (3) their counter ions are identical (i.e., cyclopentadienyl anions, Cp^-), (4) cyclopentadienyl anions exhibit no fire suppression effect, and (5) these metallocenes easily decompose at elevated temperatures because the bond dissociation energy of metal–Cp ring bonds is low [11]. These factors allow a direct comparison of the inhibition abilities of transition metals and the results of such testing have indicated that the relative suppression effects of these compounds can be ordered as: $CrCp_2 > MnCp_2 > FeCp_2 > CoCp_2 > NiCp_2$ [10]. Interestingly, this progression reflects the order of the atomic number of the central metals of these compounds.

The objective of the present study was to systematically and directly compare the inhibition efficiency of transition metals by employing three metallocenes: ruthenocene ($RuCp_2$), osmocene ($OsCp_2$), and vanadocene (VCp_2). Ruthenium and osmium belong to the same group in the periodic table as iron (Group 8), while vanadium is in the same period as chromium, manganese, iron, cobalt, and nickel (Period 4). Thus, the influence on fire suppression ability of both the group and the period in the periodic table was investigated. The fire suppression ability of a flame inhibitor is typically

evaluated using a cup burner flame [12]; however, the experiments in this study were carried out by combusting a filter paper on which the metallocene was adsorbed, owing to the very low vapor pressures of these compounds. In the combustion experiments, the downward flame spread rate was measured to determine whether the metallocene produced its flame inhibition effect. Downward flame spreading over the filter-paper samples used in this study resulted from the transfer of sufficient heat from the flame to the thermally thin cellulosic fuel, since this heat transfer was sufficient to produce combustible gases from the cellulose through a pyrolysis process [13]. The flame spread rate could potentially be reduced in cases in which the metallocene produced a flame inhibition effect when in the gas phase. If the metallocene in its solid phase hampered the decomposition of the cellulose, the production of combustible gases was inhibited, resulting in a decrease in the flame spread rate. These mean that the combustion experiments alone was not enough to determine the phase in which the metallocene exerts its flame inhibition effect, since both the gas- and solid-phase flame inhibition effects would be observed in such trials. The determination of the phase is of great importance in terms of understanding the inhibition mechanisms. In this study, in addition to the combustion trials, the metallocenes were evaluated with regard to their flame inhibition efficiency in the solid phase using thermogravimetric analysis (TGA) in order to finally determine the phase, gas and/or solid, in which the metallocene generated its suppression effect. Cheng et al. performed TG measurements in air to determine the kinetic parameters

associated with the combustion of cellulose, including the activation energy (E_a) and pre-exponential factor (A) [14]. The present study evaluated the metallocenes with regard to their solid phase flame inhibition abilities by comparing the kinetics parameters (that is, the activation energy and pre-exponential factor) and char yields of various metallocene/cellulose systems with those for pure cellulose.

2. Material and methods

2.1 Chemicals and materials

$RuCp_2$ (purity > 99%), $OsCp_2$ (purity > 99%), and VCp_2 (purity > 95%) (see Fig. 1 for molecular structures) were purchased from Strem Chemicals, Inc. (Newburyport, MA, USA). All three commercially available metallocenes were employed as-received. Dehydrated solvents (toluene and *n*-hexane, purity > 99.5%) were purchased from the Kanto Chemical Co., Inc. (Tokyo, Japan) and filter paper with a uniform thickness of 0.18 mm and a density of 87 g/m^2 was obtained from Tokyo Roshi Kaisha, Ltd. (Tokyo, Japan).

2.2 Flame spread rate measurements

Flame spread rates on filter papers were measured to evaluate the fire suppression ability of each

of the metallocenes. A filter paper made from natural cellulose was utilized as a typical combustible solid. The paper was cut into rectangular shapes (5.0 mm wide × 120.0 mm long) using Teflon-coated scissors. After drying in a desiccator for 48 h, the paper sections were weighed in a dry glovebox filled with dry nitrogen (> 99.99%). The cut paper was subsequently immersed in a toluene solution of the metallocene for 15 min. The exception was VCp_2, which was instead dissolved in *n*-hexane since it is completely insoluble in toluene. The cut paper was then allowed to dry in a desiccator and was again weighed. In this manner, filter paper samples on which the metallocenes were homogeneously adsorbed were prepared. The amount of metallocene adsorbed per unit weight of the cut paper, *C*, can be expressed by the following equation:

$$C = (W_s - W_0) / W_0 / M \quad (1)$$

where W_s is the weight of the sample, W_0 is the dry weight of the cut paper and M is the molar mass of the metallocene. That is, C is the concentration of the metallocene on the rectangular paper sample.

The experimental setup was adopted from our previous study [10] and is shown in Fig. 2. Each prepared sample was fixed on a sample holder in an acrylic tube (80 mm in diameter × 300 mm in height), after which dry air was passed upward at a flow rate of 5.0 L/min. The filter paper samples

were sufficiently sturdy such that they remained positioned vertically without any requirement for support. In this work, fire suppression by the metallocene was characterized based on downward flame spread rate over the sample. For each experimental trial, the sample was ignited at its upper edge with a pilot flame. To remove any effect of the pilot flame, the downward flame spread rate was determined by measuring the time during which the flame propagated from a point 10 mm below the top of the sample to a point 80 mm below the top. The normalized flame spread rate, V, is defined as

$$V = U_s / U_0 \qquad (2)$$

where U_s is the flame spread rate measured for the sample and U_0 (mm/s) is the flame spread rate observed for the pure cut paper without any metallocene (mm/s).

2.3 Thermogravimetric (TG) measurements

Thermogravimetric tests were performed to examine the thermal behavior of the metallocene and to calculate the apparent activation energies and pre-exponential factors associated with the pyrolysis of cellulose powders mixed with the metallocene using the Kissinger method [15]. In addition, the char yields at 873 K were also determined by TGA. TG experiments were conducted with a

thermogravimetric analyzer (Shimadzu TGA-50, Japan) calibrated with indium, tin, and zinc as reference materials. In these trials, metallocene powders were milled with powdered cellulose (< 20 μm) prior to analysis. After drying in a desiccator filled with dry nitrogen gas, approximately 3 mg of the sample was loaded into a test crucible. In this study, aluminum crucibles were employed since there were no significant differences in thermal behavior observed between samples in aluminum and alumina crucibles. The purge gas was dry air at a flow rate of 50 mL/min and TG runs were carried out at linear heating rates of 5, 10, 15 and 20 K/min over the temperature range of 298–873 K. When the reaction order was 1, the activation energy and pre-exponential factor were calculated using the Kissinger expression:

$$\ln (\beta/T^2_{max}) = -E_a/RT_{max} + \ln (AR/E_a) \quad (3)$$

where β is the heating rate ($\beta = dT/dt$), T_{max} is the temperature at the maximum weight loss rate, and R is the ideal gas constant (8.31 J/mol K). Thus, the activation energy and pre-exponential factor can be determined from the slope of $\ln (\beta/T^2_{max})$ as a function of $1/T_{max}$ and the intercept, respectively.

The TG trials noted above were performed under air. TGA techniques have frequently been employed to investigate the combustion mechanism of cellulose in an air atmosphere, and the decomposition has been found to consist of a two-step degradation process [14, 16]. The first step,

occurring at lower temperatures (ca. 520 K), is attributed to the pyrolysis of the cellulose, while the second step at higher temperatures (> ca. 700 K) corresponds to char burning. It has also been demonstrated that the pyrolysis of cellulose is not affected by the oxygen concentration of the ambient atmosphere [17], such that there are no significant differences in the TGA data between experiments conducted under inert or air atmospheres. Thus, the TG measurements in the present study were conducted in an air atmosphere with the aim of observing both the pyrolysis and char burning processes.

2.4 X-ray diffraction (XRD)

A sample of each metallocene powder was conditioned at 473, 523, 623, or 773 K for 1 h in air prior to XRD analysis. The phase structure of each pre-conditioned sample was characterized using a Rigaku X-ray diffractometer (RINT-2500, Japan) with Cu Kα radiation.

3. Results and discussion

3.1 Flame spread rate measurements

Figs. 3a and b illustrate the normalized flame spread rates as a function of the concentration of $RuCp_2$ and $OsCp_2$, respectively. In Fig. 3, the error bars represent one standard deviation (σ_v). As can be seen from these figures, the suppression characteristics of the two metallocenes were very

similar. That is, at lower concentrations, the normalized flame spread rate gradually decreased with increases in the metallocene concentration, eventually approaching a minimum value. However, at higher metallocene concentrations, the flame spread rate is observed to increase, meaning that the flame inhibiting effects of these metallocenes on the filter paper combustion were diminished. The normalized flame spread rate of the ruthenocene sample exhibited a minimum at a concentration of 4.96×10^{-5} mol/g, and the minimum normalized flame spread rates of the $RuCp_2$ and $OsCp_2$ samples were determined to be 0.85 and 0.87, respectively. Within the concentration range tested, no glowing was observed in any of the samples.

The suppression behavior of these metallocenes is very similar to that of nickelocene and cobaltocene [10] and can likely be attributed to two factors: (1) the condensation of metal species in the gas phase and (2) the flammability of these compounds. Regarding factor (1), Rumminger and Linteris have studied the influence of the condensation of metal species in methane/air flames using $Fe(CO)_5$ as an inhibitor [18]. This research demonstrated that increasing the concentration of $Fe(CO)_5$ in the flame led to a decrease in the fire suppression effect. In addition, numerical calculations and experimental measurements showed that a large proportion of the metal species was agglomerated and condensed at high concentrations. The condensation of metal species such as ruthenium oxides and osmium oxides in flames results in a corresponding decrease in their suppression capability. With respect to factor (2), the metallocenes used in this study have two

contrasting effects: they not only have the ability to suppress filter paper combustion, but are also themselves flammable. At higher concentrations, the flammability of these metallocenes thus likely surpasses their suppression effect, reducing the apparent suppression of combustion and thereby increasing the flame spread rate.

In Fig. 3c, the normalized flame spread rates are plotted against the concentration of VCp_2. Owing to the adsorption limit of VCp_2 on the filter paper, we were unable to prepare a sample with uniform adsorption above a concentration of 7.08×10^{-4} mol/g. Within the concentration range tested, however, the normalized flame spread rate slowly decreased and approached a minimum value of $V = 0.83$. Glowing of the sample was also observed over the range of 2.48×10^{-5} to 7.08×10^{-4} mol/g. The flame spread rate (U_0) and associated standard deviation (σ_0) obtained from the combustion of untreated rectangular paper samples were 2.68 mm/s and 0.01 mm/s, respectively. There were significant differences in the normalized flame spread rates of treated samples (σ_v) between the metallocenes, excluding VCp_2, since the observed differences were greater than twice the pooled standard deviation. In contrast, no significant differences seem to be present between VCp_2 and the others, owing to the large standard deviation of the VCp_2-treated sample.

3.2 TG and XRD measurements

TG measurements were conducted to gain insight into the suppression mechanism associated with

the metallocenes used in this study. Specifically, as noted above, we investigated whether the activation energy, pre-exponential factor, and char yield were modified by the metallocenes. Comparing the activation energy and pre-exponential factor of pure cellulose powder (Ea_{cel} and A_{cel}) with those of cellulose powders containing metallocenes (Ea_s and A_s) allows an evaluation of the phase in which these metallocenes apply an inhibition effect. The metallocenes are judged to have no suppression effect in the solid phase if $Ea_s \approx Ea_{cel}$ and $A_s \approx A_{cel}$. In contrast, the observation that $Ea_s > Ea_{cel}$ and $A_s > A_{cel}$ provides evidence of a suppression effect in the solid phase. In addition, the char yield will increase when the metallocenes act as a flame inhibitor in the solid phase.

In the TG measurements, the concentrations of $RuCp_2$, $OsCp_2$, and VCp_2 were 2.73×10^{-5}, 4.96×10^{-5}, and 7.08×10^{-4} mol/g, respectively, since these were the concentration values at which these metallocenes best minimized the flame spread rates, as shown in Fig. 3. The T_{max} values of $RuCp_2$/cellulose, $OsCp_2$/cellulose, $RuCp_2$/cellulose, and pure cellulose at a heating rate of 10 K/min were found to be 604.3, 604.3, 586.3, and 604.3 K, respectively. There were thus no significant differences in the peak temperatures, indicating that thermal oxidative degradation of cellulose likely occurred by the same reaction mechanism in each case, and allowing direct comparisons of the kinetics parameters.

As shown in Fig. 4, the plots of $\ln(\beta/T^2_{max})$ versus $1/T_{max}$ provide straight lines with high coefficients of determination (≥ 0.90). The apparent activation energies obtained from the Kissinger

method are depicted in Table 1, from which it can be seen that the activation energies associated with $RuCp_2$/cellulose, $OsCp_2$/cellulose and pure cellulose were 143.9, 157.2, and 151.1 kJ/mol, respectively. Similarly, the activation energies of the $CrCp_2$/cellulose, $MnCp_2$/cellulose, $FeCp_2$/cellulose, $CoCp_2$/cellulose, and $NiCp_2$/cellulose systems were determined to be 150.7, 149.8, 150.2, 150.5, and 150.7 kJ/mol, respectively. The logarithms of the pre-exponential factors of the $RuCp_2$/cellulose, $OsCp_2$/cellulose, $CrCp_2$/cellulose, $MnCp_2$/cellulose, $FeCp_2$/cellulose, $CoCp_2$/cellulose, and $NiCp_2$/cellulose systems, and of pure cellulose were 12.09, 13.28, 11.09, 11.08, 11.76, 11.49, 11.94, and 11.19, respectively. The values of Ea_{cel} and A_{cel} derived in this manner were in excellent agreement with those reported in the literature [14]. In addition, the char yields were found to be approximately zero. There were thus no significant differences in the values of the activation energies, pre-exponential factors, and char yields between the treated samples and the pure cellulose. These data and the combustion experiments described in Section 3.1 indicate that these metallocenes, excluding VCp_2, produce a flame inhibition effect not in the solid phase but rather in the gas phase. In contrast, unlike the other metallocenes, the E_a, A, and char yield of the VCp_2/cellulose system were 278.9 kJ/mol, 18.59, and 24.5%, respectively; thus, VCp_2 significantly enhanced the activation energy, pre-exponential factor, and char yield and therefore exerted a flame inhibition effect in the solid phase.

To understand the distinctly different behavior of vanadocene from other metallocenes, TG

measurements of VCp_2 were conducted under an air flow. Fig. 5 shows the TG curves obtained from VCp_2 and $FeCp_2$ as a function of temperature. In general, the metallocenes including $FeCp_2$, $RuCp_2$, $OsCp_2$, $CrCp_2$, $MnCp_2$, $CoCp_2$ and $NiCp_2$ begin to sublime below about 400 K. As shown in this figure, the TG curve of $FeCp_2$ exhibited one weight loss stage over the temperature range of about 350 to 450 K without any residual material. In contrast, the TG curve of VCp_2 had several weight-loss stages, while the major weight loss of about 40% was observed over 675 K, leaving a yellow residue equal to about 50% of the original mass. The XRD pattern of VCp_2 heated at 773 K in air revealed that this yellow solid was vanadium pentoxide (see Fig. 6). Hence, the weight loss at > 675 K corresponds to the formation of vanadium pentoxide. It is probable that vanadium pentoxide was produced via vanadium oxides with low oxidation states. The 10% weight loss observed in the 400–650 K range may be due to the oxidation of VCp_2 into vanadium oxides with lower oxidation states, including +2, +3, and +4. Unfortunately, the XRD patterns of VCp_2 heated at 473, 523 or 623 K did not allow the identification of specific vanadium oxides because of the broad spectra associated with these compounds. Since cellulose starts to decompose at ca. 540 K, the results indicate that these nonvolatile vanadium oxides, including vanadium pentoxide, likely act as flame inhibitors in the solid phase.

3.3 Ranking of the transition metals

Table 2 summarizes the suppression efficiency data obtained from the present study, together with the data for $CrCp_2$, $MnCp_2$, $FeCp_2$, $CoCp_2$, and $NiCp_2$ from our preceding study [10]. In this table, the minimum normalized downward flame spread rates of the rectangular filter paper samples on which the metallocenes were adsorbed are listed. In addition, the extinguishing concentrations associated with $CrCp_2$, $MnCp_2$, and $FeCp_2$ are provided, since these compounds were able to completely extinguish the flame as described above. As can be seen from Table 2, the ranking of their inhibition effect is as follows: Cr > Mn > Fe > Co > Ni > (V) > Os > Ru. It is evident from this ranking that there is no clear correlation between inhibition ability and the position of the metal in terms of its group and period in the periodic table.

Rumminger et al. suggested that the inhibition reactions of metallic compounds in the gas phase occur by two reaction pathways: decomposition of the metallic compound to generate metal atoms and conversion of the metal atoms to metal oxides via a homogeneous catalytic cycle [5]. The metallocenes readily decompose to generate the corresponding transition metal even at relatively low temperatures because of the weak coordinate bonds between the central metal and the cyclopentadienyl rings. Thus suppression of the filter paper fires is most likely dominated by two factors: (1) the amount of metallic species introduced into the flame and (2) the ability of these species to undergo radical recombination in the flame. In other words, factor (1) is a physical effect, while factor (2) represents a chemical process.

The inhibition effect is remarkably affected by the concentration of inhibiting species, such as metals or metal oxides, in the flame because inhibiting species in excess of the superequilibrium concentration are effective at recombining radicals [8, 19]. Unfortunately, in this study, it was difficult to accurately determine the concentration of inhibiting species added into flames over the filter papers. As noted, the addition of metal elements into the flame is of great importance as the first step in the catalytic radical recombining cycle. For this reason, we examined the vapor pressures of these metals, since the amount of each metal introduced into the flame should have a positive correlation with its vapor pressure. It was expected that higher metal vapor pressures would be correlated with more effective gas-phase radical recombination. In Fig. 7, the vapor pressures of these metals are plotted against temperature. Vapor pressure is the equilibrium pressure at a given temperature and the flame temperatures may vary depending on the metallocene adsorbed because the inhibition efficiency greatly depends on the transition metal. Here, however, we simply assume a flame temperature of ca. 1100 K, which is the surface temperature of plain filter paper during combustion [20]. Alcock et al. have proposed a four-term equation for the vapor pressures of metals as a function of temperature [21] that exhibits better than ± 1% accuracy over the temperature range of 298 to 2500 K. The equations is

$$\log P\,(\text{atm}) = A + B/T + C \log T + DT/1000 \qquad (4)$$

where *P* is the metal vapor pressure and A–D are coefficients. The vapor pressures of ruthenium, osmium, and vanadium calculated from Equation (4) are shown in Fig. 7, along with the vapor pressures of chromium, manganese, iron, cobalt, and nickel. As can be seen from Fig. 7, the vapor pressures of the metals at a temperature of ca. 1100 K are as follows: Mn: 4.3×10^{-7}, Cr: 1.9×10^{-11}, Fe: 5.4×10^{-12}, Co: 2.1×10^{-13}, Ni: 2.3×10^{-13}, V: 2.5×10^{-17}, Ru: 1.9×10^{-23}, and Os: 6.0×10^{-30} atm. Their metal vapor pressures therefore increase in order of Mn > Cr > Fe > Co ≈ Ni > V > Ru > Os.

Accordingly, the ranking of the flame suppression abilities of these metals is in good agreement with the order of their vapor pressures. Hence, factor (1) (i.e., metal vapor pressure) represents the key parameter influencing the inhibition effect. However, the flame suppression order does not completely coincide with the order of the metal vapor pressures in terms of the placements of Mn and Cr as well as Os and Ru. This discrepancy could be due to the effect of factor (2). In fact, the molar extinction concentration of $CrCp_2$ for filter paper combustion was only two times less than that of $MnCp_2$ [10], notwithstanding the fact that the vapor pressure of Cr at 1100 K is four orders of magnitude lower than that of Mn. This implies that Cr has a relatively pronounced ability to scavenge radicals in flames. Further studies may be needed to elucidate the inhibition efficiency and mechanisms of other metals.

4. Conclusions

By employing a series of metallocenes, this study directly and systematically compared the flame inhibition abilities of a number of transition metals: vanadium, ruthenium, osmium, chromium, manganese, iron, cobalt, and nickel. On the basis of the results presented in this paper, the following conclusions can be drawn:

1. The minimum normalized flame spread rates over rectangular filter paper samples on which vanadocene, osmocene, or ruthenocene had been homogeneously adsorbed are determined to be 0.83, 0.85, and 0.87, respectively. None of these compounds was able to extinguish combustion of the filter paper, whereas chromocene, manganocene, and ferrocene were able to do so.
2. The experimental data show that the transition metals can be ranked in the following order in terms of their combustion inhibition properties: Cr > Mn > Fe > Co > Ni > (V >) Os > Ru.
3. Thermogravimetric measurements demonstrated that the activation energies, pre-exponential factors, and char yields of the metallocene/cellulose systems, with the exception of vanadocene/cellulose, do not significantly differ with those of pure cellulose. In contrast, the kinetic parameters and char yield of vanadocene/cellulose are remarkably high compared to those of pure cellulose.

4. The filter paper combustion trials and the subsequent thermogravimetric analysis provide insight into the flame inhibition mechanism. Chromocene, manganocene, ferrocene, cobaltocene, nickelocene, ruthenocene, and osmocene all produce a flame inhibition effect in the gas phase, while vanadocene exhibits suppression in the solid phase. The unique inhibition properties of vanadocene are likely due to the formation of stable, nonvolatile vanadium oxides, including vanadium pentoxide, from vanadocene.

Acknowledgment

XRD measurements were conducted at the Instrumental Analysis Center of Yokohama National University. This work was financially supported by JST A-STEP Grant Number AS242Z02524M and JSPS KAKENHI Grant Number 25750135.

References

[1] P. Joseph, E. Nichols, V. Novozhilov, A comparative study of the effects of chemical additives on the suppression efficiency of water mist, Fire Saf. J. 58 (2013) 221–225.

[2] H. Ohtani, Y. Ueno, Y. Koshiba, Experimental study on fire extinguishing ability of iron compounds and manganese chloride, Proc. Asia Pac. Symp. Saf. 7 (2011) 81–84.

[3] G.T. Linteris, V.D. Knyazev, V.I. Babushok, Inhibition of premixed methane flames by

manganese and tin compounds, Combust. Flame 129 (2002) 221–238.

[4] E.M. Bulewicz, P.J. Padley, D.H. Cotton, D.R. Jenkins, Metal-additive-catalysed radical-recombination rates in flames, Chem. Phys. Lett. 9 (1971) 467–468.

[5] M.D. Rumminger, D. Reinelt, V. Babushok, G.T. Linteris, Numerical study of the inhibition of premixed and diffusion flames by iron pentacarbonyl, Combust. Flame 116 (1999) 207–219.

[6] I.E. Gerasimov, D.A. Knyazkov, A.G. Shmakov, A.A. Paletsky, V.M. Shvartsberg, T.A. Bolshova, O.P. Korobeinichev, Inhibition of hydrogen–oxygen flames by iron pentacarbonyl at atmospheric pressure, Proc. Combust. Inst. 33 (2011) 2523–2529.

[7] M.R. Agrawal, C. Winder, Frequency and occurrence of LD_{50} values for materials in the workplace, J. Appl. Toxicol. 16 (1996) 407–422.

[8] G.T. Linteris, M.D. Rumminger, K. Babushok, W. Tsang, Flame inhibition by ferrocene and blends of inert and catalytic agents, Proc. Combust. Inst. 28 (2000) 2965–2972.

[9] G.T. Linteris, M.D. Rumminger, V.I. Babushok, Catalytic inhibition of laminar flames by transition metal compounds, Prog. Ener. Combust. Sci. 34 (2008) 288–329.

[10] Y. Koshiba, Y. Takahashi, H. Ohtani, Flame suppression ability of metallocenes, Fire Saf. J. 51 (2012) 10–17.

[11] M.J. Mayor-Lopez, J. Webe, DFT calculations of the binding energy of metallocenes, Chem. Phys. Lett. 281 (1997) 226–232.

[12] G.T. Linteris, V.R. Katta, F. Takahashi, Experimental and numerical evaluation of metallic compounds for suppressing cup-burner flames, Combust. Flame 138 (2004) 78–96.

[13] C.D. Blasi, Processes of flames spreading over the surface of charring fuels: Effects of the solid thickness, Combust. Flame 97 (1994) 225–239.

[14] K. Cheng, W.T. Winter, A.J. Stipanovic, A modulated-TGA approach to the kinetics of lignocellulosic biomass pyrolysis/combustion, Polym. Degrad. Stabil. 97 (2012) 1606–1615.

[15] I. Brnardić, J. Macan, H. Ivanković, M. Ivanković, Thermal degradation kinetics of epoxy/organically modified montmorillonite nanocomposites, J. Appl. Polym. Sci. 107 (2008) 1932–1938.

[16] M. Amutio, G. Lopez, R. Aguado, M. Artetxe, J. Bilbao, M. Olazar, Kinetic study of lignocellulosic biomass oxidative pyrolysis, Fuel 95 (2012) 305–311.

[17] D. Shen, J. Ye, R. Xiao, H. Zhang, Carbohydr. Polym. 98 (2013) 514–521.

[18] M.D. Rumminger, G.T. Linteris, The role of particles in the inhibition of premixed flames by iron pentacarbonyl, Combust. Flame 123 (2000) 1932–1938.

[19] V. Babushok, W. Tsang, G.T. Linteris, D. Reinelt, Chemical limits to flame inhibition, Combust. Flame 115 (1998) 551–560.

[20] T. Hirano, S.E. Norekis, T.E. Waterman, Measured velocity and temperature profiles near flames spreading over a thin combustible solid, Combust. Flame 138 (1974) 83–96.

[21] C.B. Alcock, V.P. Itkin, M.K. Horrigan, Vapor pressure equations for the metallic elements: 298–2500 K,. Can. Metall. Quart. 23 (1984) 309–313.

Figure captions

Fig. 1 Chemical structures of vanadocene, ruthenocene, osmocene, chromocene, manganocene, ferrocene, cobaltocene, and nickelocene.

Fig. 2 (a) Experimental apparatus for assessment of filter combustion and (b) a photographic image of ruthenocene-treated paper sample during combustion.

Fig. 3 Normalized flame spread rates as a function of the concentration of (a) ruthenocene, (b) osmocene, and (c) vanadocene. Closed symbols: combustion; open symbols: glowing. Error bars indicate ± one standard deviation.

Fig. 4 Kissinger plots for experimental data obtained at heating rates of 5, 10, 15, and 20 K/min. Legend: ■ = vanadocene. ● = ruthenocene, ▲ = osmocene.

Fig. 5 TG curves for vanadocene (○) and ferrocene (□) obtained at a heating rate of 10 K/min under an air flow. The inset shows a photographic image of the yellow solid formed from vanadocene at 873 K.

Fig. 6 X-ray diffraction patterns of (a) vanadium pentoxide and (b) vanadocene powders heated for 1 h in air.

Fig. 7 Vapor pressure values of metals as a function of temperature (adapted from ref. [21]).

Table captions

Table 1 Apparent activation energies, pre-exponential factors, and char yields of the metallocene/cellulose systems and of pure cellulose.

Table 2 Minimum normalized flame spread rates and extinguishing concentrations obtained with various metallocenes.

Table 1

Sample	*E* (kJ/mol)	$\log_{10}$ (*A* (1/min))	Char yield [a] (%)
Vanadocene/cellulose	278.9	18.59	24.5
Ruthenocene/cellulose	143.9	12.09	2.1
Osmocene/cellulose	157.2	13.28	0
Nickelocene/cellulose	150.7	11.94	0
Cobaltocene/cellulose	150.5	11.49	0
Ferrocene/cellulose	150.2	11.76	0
Manganocene/cellulose	149.8	11.08	0
Chromocene/cellulose	150.7	11.09	0
Pure cellulose	151.1	11.19	0

a: at 873 K.

Table 2

Metallocene	Minimum V [a]	Extinguishing concentration ($\times 10^{-4}$ mol/g) [b]
Ruthenocene	0.87	ND[c]
Osmocene	0.85	ND[c]
Vanadocene	0.83	ND[c]
Nickelocene [10]	0.34	ND[c]
Cobaltocene [10]	0.25	ND[c]
Ferrocene [10]	0	0.50
Manganocene [10]	0	0.15
Chromocene [10]	0	0.07

a: normalized flame spread rate over a rectangular filter paper sample on which the metallocene has been adsorbed; b: concentration of the metallocene on the filter paper; c: not detected.

Figure 1

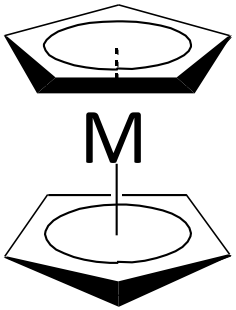

M = V : vanadocene
Ru : ruthenocene
Os : osmocene
Cr : chromocene
Mn : manganocene
Fe : ferrocene
Co : cobaltocene
Ni : nickelocene

Figure 2

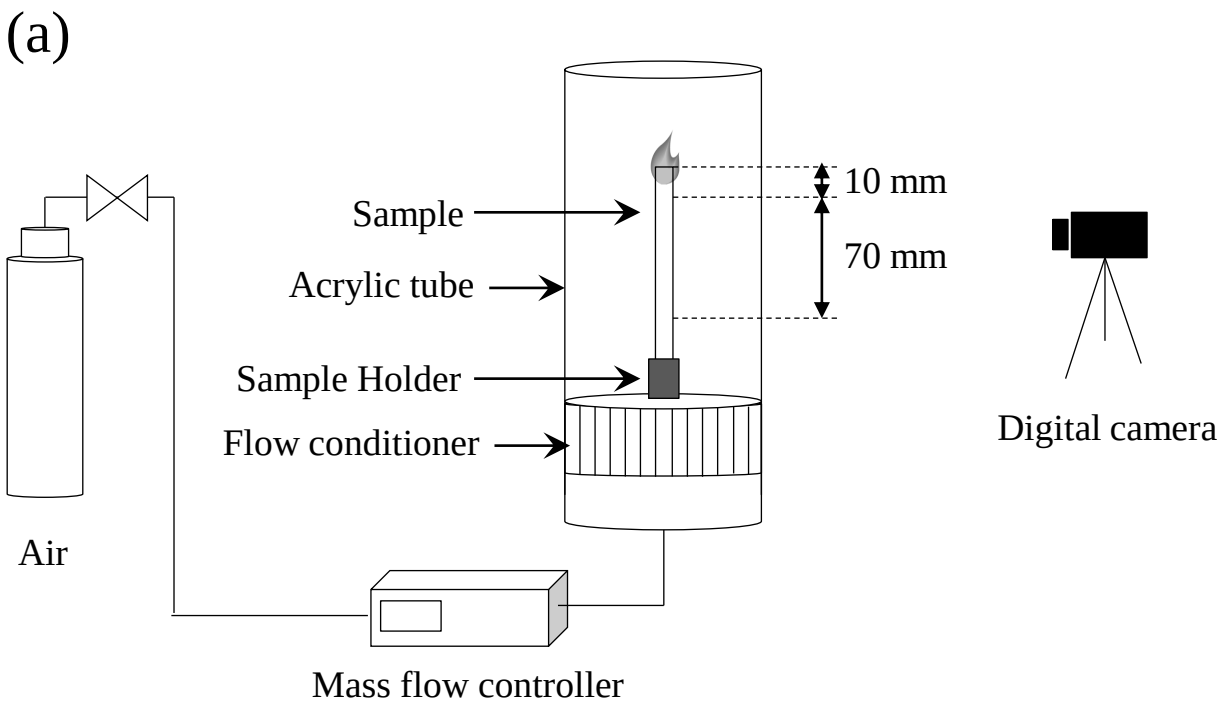
(a)
Sample
Acrylic tube
Sample Holder
Flow conditioner
10 mm
70 mm
Digital camera
Air
Mass flow controller
(b)

Figure 3

Figure 3a

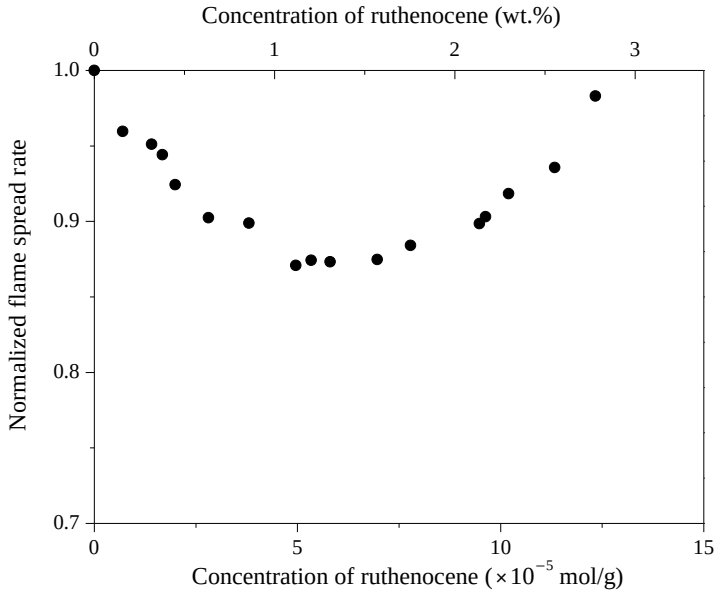

Figure 3b

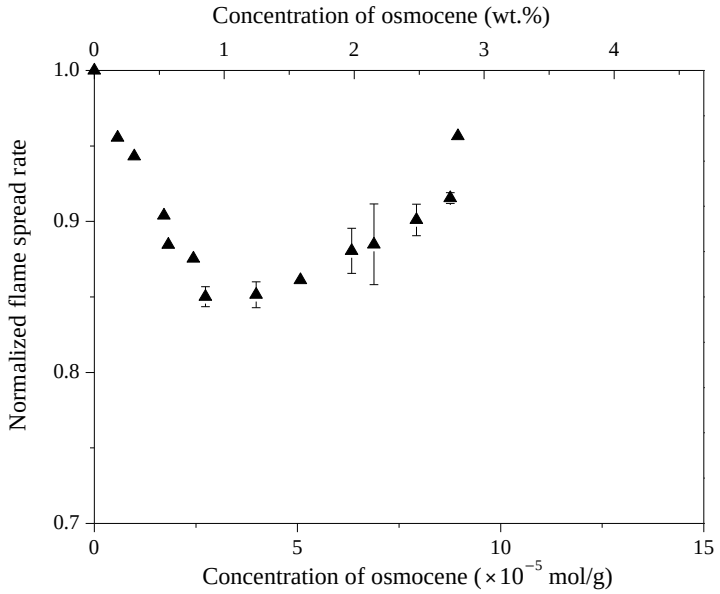
Concentration of osmocene (wt.%)
0
1
2
3
4
1.0
0.9
0.8
0.7
Normalized flame spread rate
0
5
10
15
Concentration of osmocene (×10⁻⁵ mol/g)

Figure 3c

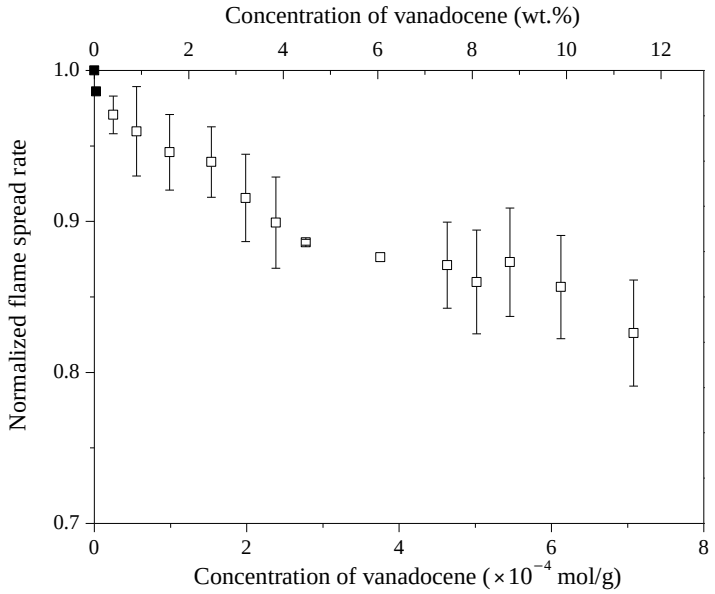
Concentration of vanadocene (wt.%)
0
2
4
6
8
10
12
1.0
0.9
0.8
0.7
Normalized flame spread rate
0
2
4
6
8
Concentration of vanadocene (×10^{-4} mol/g)

Figure 4

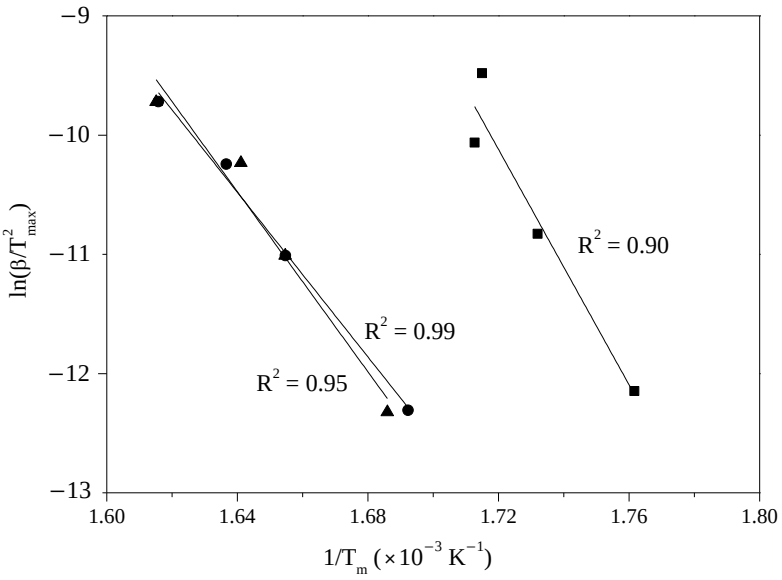
−9
−10
−11
−12
−13
1.60
1.64
1.68
1.72
1.76
1.80
ln(β/T²max)
1/Tm (×10⁻³ K⁻¹)
R² = 0.99
R² = 0.95
R² = 0.90

Figure 5

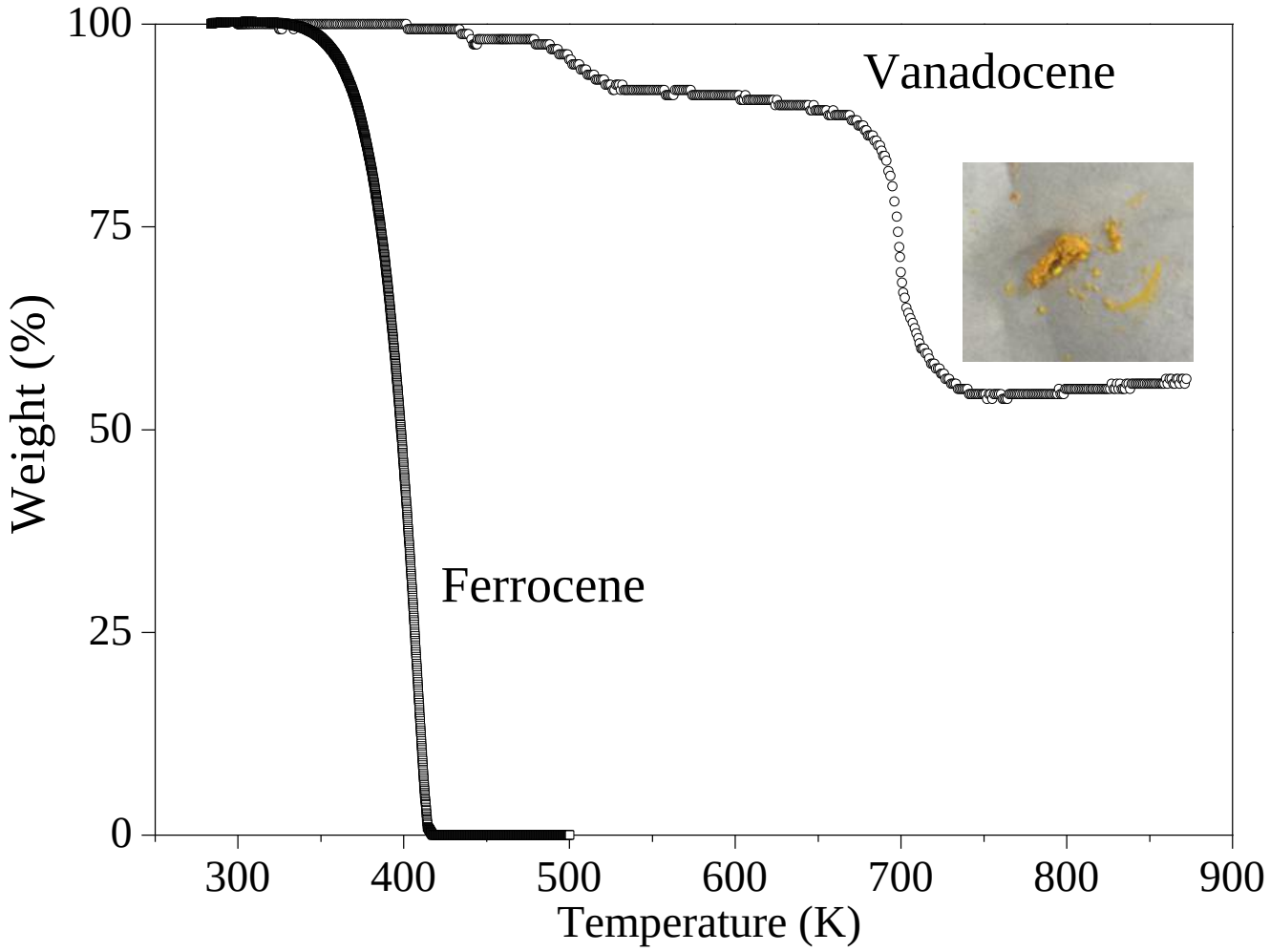
100
75
50
25
0
Weight (%)
300
400
500
600
700
800
900
Temperature (K)
Vanadocene
Ferrocene

Figure 6

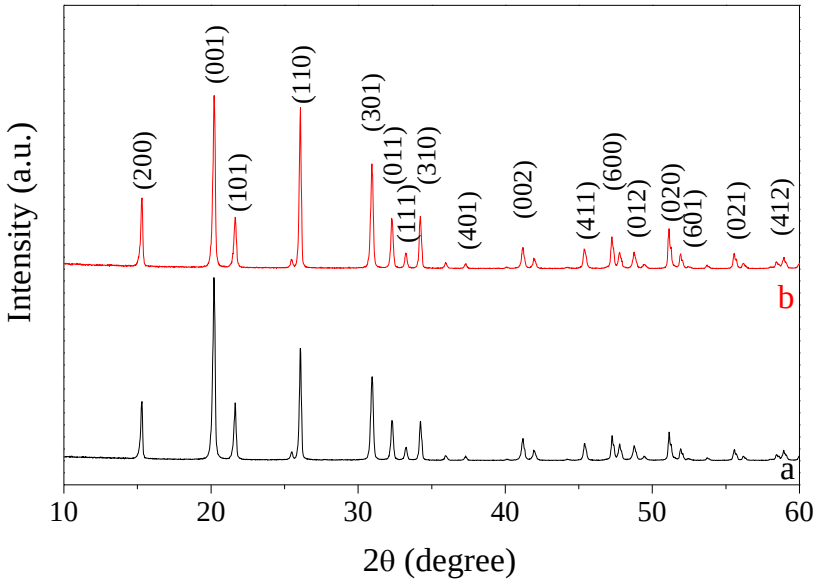
Intensity (a.u.)
(200)
(001)
(101)
(110)
(301)
(011)
(111)
(310)
(401)
(002)
(411)
(600)
(012)
(020)
(601)
(021)
(412)
b
a
10
20
30
40
50
60
2θ (degree)

Figure 7

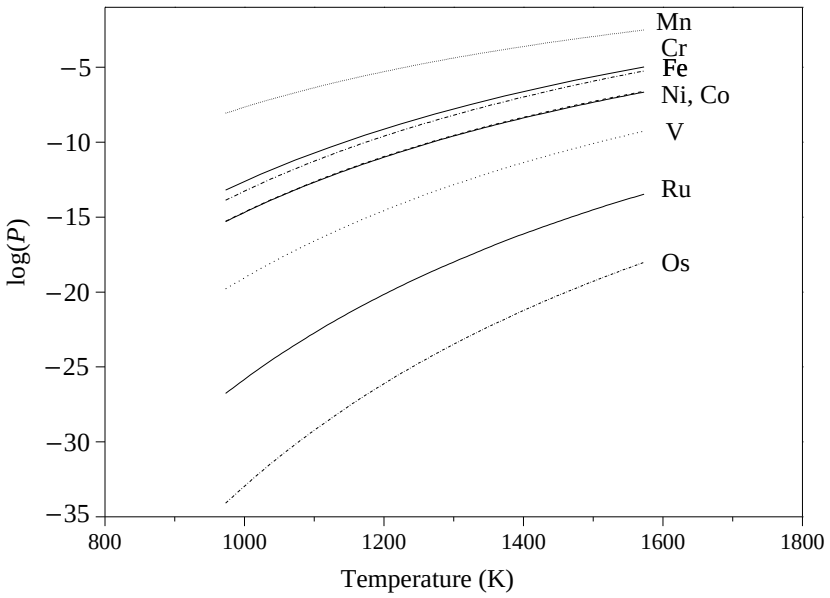
Mn
Cr
Fe
Ni, Co
V
Ru
Os
log(P)
−5
−10
−15
−20
−25
−30
−35
800
1000
1200
1400
1600
1800
Temperature (K)

Highlights

- The flame inhibition effects of transition metals are evaluated using metallocenes.
- Solid phase inhibition efficiencies are determined by thermogravimetric analysis.
- The abilities of the metals can be ranked as: Cr > Mn > Fe > Co > Ni > (V >) Os > Ru.